Influence of spin-orbit and spin-Hall effects on the spin-Seebeck current beyond linear response: A Fokker-Planck approach

L. Chotorlishvili,[1] Z. Toklikishvili,[2] X.-G. Wang,[3] V. K. Dugaev,[4] J. Barnaś,[5,6] and J. Berakdar[1]

[1]*Institut für Physik, Martin-Luther Universität Halle-Wittenberg, D-06120 Halle/Saale, Germany*

[2]*Faculty of Exact and Natural Sciences, Tbilisi State University, Chavchavadze Avenue 3, 0128 Tbilisi, Georgia*

[3]*School of Physics and Electronics, Central South University, Changsha 410083, China*

[4]*Department of Physics and Medical Engineering, Rzeszow University of Technology, 35-959 Rzeszow, Poland*

[5]*Faculty of Physics, Adam Mickiewicz University, ulica Umultowska 85, 61-614 Poznań, Poland*

[6]*Institute of Molecular Physics, Polish Academy of Sciences, ulica M. Smoluchowskiego 17, 60-179 Poznań, Poland*

(Received 15 October 2018; revised manuscript received 20 December 2018; published 10 January 2019)

We study the spin transport theoretically in heterostructures consisting of a ferromagnetic metallic thin film sandwiched between heavy-metal and oxide layers. The spin current in the heavy-metal layer is generated via the spin Hall effect, whereas the oxide layer induces at the interface with the ferromagnetic layer a spin-orbital coupling of the Rashba type. Impact of the spin-Hall effect and Rashba spin-orbit coupling on the spin-Seebeck current is explored with a particular emphasis on nonlinear effects. Technically, we employ the Fokker-Planck approach and contrast the analytical expressions with full numerical micromagnetic simulations. We show that, when an external magnetic field H_0 is aligned parallel (antiparallel) to the Rashba field, the spin-orbit coupling enhances (reduces) the spin pumping current. In turn, the spin-Hall effect and the Dzyaloshinskii-Moriya interaction are shown to increase the spin pumping current.

DOI: 10.1103/PhysRevB.99.024410

I. INTRODUCTION

In a seminal paper [1], Bychkov and Rashba explored the impact of spin-orbit (SO) interaction on the properties of two-dimensional semiconductor heterostructures. Since then, the basic idea of Bychkov and Rashba was carried over to other research areas of physics. It was shown, for instance, that the SO interaction plays a significant role in the quantum spin-Hall effect (SHE) in graphene [2], in Bose-Einstein condensates [3], and in the orbital-based electron-spin control [4]. Recent experiments [5,6] revealed the role of SO interaction in the motion of domain walls as well. Combining the SO coupling and thermal effects bring in new insights and phenomena. A thermal bias applied to a ferromagnetic insulator leads to the formation of a thermally assisted magnonic spin current that is proportional to the temperature gradient. This phenomenon falls in the class of spin-Seebeck effects (SSEs) and may be useful for thermal control of magnetic moments [7–23]. The objective of this paper is to study the impact of SO interaction on the formation and transport of thermally assisted magnonic spin current in spin-active multilayers. We investigate two different heterostructures which include a layer of ferromagnetic metal sandwiched between heavy-metal and oxide materials, see Figs. 1 and 2. In both cases, an inversion asymmetry is caused by two different interfaces—heavy-metal/ferromagnet and ferromagnet/oxide ones. A large SO coupling is present in the heavy metals [24–28]. This paper is motivated by the experimental work in Ref. [27] with particular attention to the systems $Pt/Co/AlO_x$ and Ta/CoFeB/MgO [29]. Moreover, the torques generated by strong SO coupling are generally different from the Slonczewski's spin-transfer torque [1,24,30], with the prospect for novel physical effects in the heavy-metal/ferromagnetic-metal/oxide heterostructures. An applied electric voltage (see Fig. 1) generates charge current in the ferromagnetic and heavy-metal layers. This current in the heavy-metal layer leads to spin current due to the spin-Hall effect, which is then injected into the thin ferromagnetic layer [25,26,31–36] and acts as an extra torque on the localized magnetic moments in the ferromagnet. The induced torque influences the magnetization dynamics, which is the topic of this paper. To describe the influence of the spin current on the magnetization dynamics in the ferromagnetic layer, we add a relevant term to the Landau-Lifshitz-Gilbert (LLG) equation. In turn, the Rashba SO coupling at the ferromagnet/oxide interface in the presence of the charge current results in a spin polarization at the interface with the exchange coupling exerting a torque on the ferromagnetic layer as well. Thus, the SHE and the Rashba SO coupling influence the magnetization dynamics in the ferromagnetic layer through the Rashba and SHE torques, both incorporated into the LLG equation (the Rashba and SHE fields). The considered setup allows to formally investigate the interplay/competition of the torques due to Rashba SO interaction and the SH effect. The Rashba SO torque acts fieldlike, whereas the torque due to the spin current generated *via* the spin-Hall effect is predominantly damping-like/antidampinglike in nature. We utilize the Fokker-Planck method [37] for the stochastic LLG equation for studying the magnetic dynamics beyond the linear-response regime. The influence of the Rashba-type SO coupling on the magnonic spin current was studied in the works [38–40].

In the system shown in Fig. 1, the normal metal with temperature T_N is attached to the ferromagnet with $T_F > T_N$.

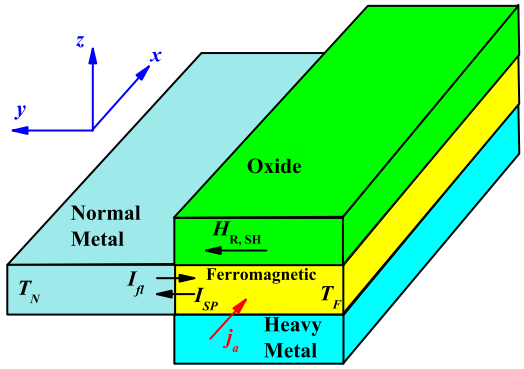

FIG. 1. Schematic of the system. A ferromagnetic metallic layer is sandwiched between the oxide and the heavy-metal layers. The injected current j_a flows in the ferromagnetic and heavy-metal layers in the x direction. The Rashba field H_R and the spin-Hall field are oriented along the y axis. The normal metal with the temperature T_N is attached to the ferromagnetic layer. The temperature of the ferromagnetic layer T_F is different from T_N.

We consider the spin current flowing from the ferromagnetic to a normal-metal layer. Magnons from the high-temperature region diffuse to the lower-temperature part giving rise to a magnonic spin current and thus to the SSE [41–43]. Magnonic spin current pumped from the ferromagnet into the normal-metal I_{sp} increases with the temperature difference $I_{sp} \sim T_F - T_N$. However, the spin current injected from the ferromagnetic layer to the normal metal is not the only spin current that crosses the normal-metal/ferromagnet interface. The fluctuating spin current I_{fl} is generated in the normal metal and flows towards the ferromagnet, i.e., in the direction opposite to the magnonic spin pumping current. The quantity of interest is therefore the total spin current $I_{\rm tot} = I_{sp} + I_{fl}$ that crosses the normal-metal/ferromagnet interface. We show that $I_{\rm tot}$ is drastically influenced by the proximity of the heavy metal (due to the spin-Hall effect) and the oxide (due to the Rashba spin-orbit coupling). In the second system (see Fig. 2) an additional normal-metal layer is attached to the ferromagnetic one.

The paper is organized as follows. In Sec. II we introduce the model under consideration. In Secs. III and IV we explore the spin current in two different heterostructures. For the sake

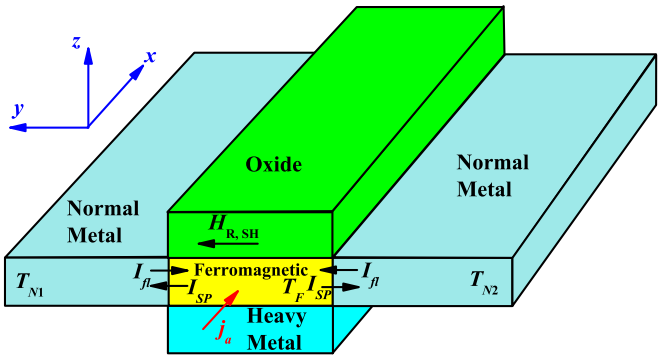

FIG. 2. Schematic of the $N/F/N$ system. The ferromagnetic film is attached to two nonmagnetic layers N_1 on the left side and N_2 on the right side. The temperatures of the layers N_1 and N_2 are different. The other notation as in Fig. 1.

of simplicity, we neglect the Dzyaloshinskii-Moriya interaction (DMI). Effects of the DMI term and magnetocrystalline anisotropy are explored numerically by micromagnetic simulations and are described in Sec. V. Section VI summarizes the findings. The main technical details are deferred to the appendices.

II. THEORETICAL MODEL

For the heavy-metal/ferromagnetic-metal/oxide sandwich we choose the ferromagnetic metallic layer to be in direct contact with a nonmagnetic metallic layer as shown in Fig. 1. We also assume that, due to a strong electron-phonon interaction, the local thermal equilibrium between electrons and phonons in both ferromagnetic and normal-metal layers is established $T_F^p = T_F^e = T_F$ and $T_N^p = T_N^e = T_N$. The magnon temperature T_F^m in the ferromagnetic layer differs, in general, from the temperature of electrons/phonons $T_F^m \neq T_F$ [43].

At nonzero temperatures, the thermally activated magnetization dynamics in the ferromagnet gives rise to a spin current flowing into the normal metal. This effect is known as spin pumping [41,44–46]. The corresponding expression for the spin current density reads [43,47]

$$\mathbf{I}_{sp}(t) = \frac{\hbar}{4\pi}[g_r \mathbf{m}(t) \times \dot{\mathbf{m}}(t) + g_i \dot{\mathbf{m}}(t)], \tag{1}$$

where g_r and g_i are the real and imaginary parts of the dimensionless spin mixing conductance of the ferromagnet/normal-metal $(F|N)$ interface, whereas $\mathbf{m}(t) = \mathbf{M}(t)/M_s$ is the dimensionless unit vector along the magnetization orientation (here, M_s is the saturation magnetization) and $\dot{\mathbf{m}} \equiv d\mathbf{m}/dt$. The spin current is a tensor describing the spatial distribution of the current flow and orientation of the flowing spin (magnetic moment). Due to the geometry of the system under consideration, the spin current flows along the y axis, see Fig. 1. In turn, the spin polarization of the current depends on the orientation of the magnetic moment and its time derivative. The average spin depends on the ground-state magnetic order which in our case is collinear with the external magnetic field (applied along the y axis). Therefore, the only nonzero component of the average spin current tensor is I_{sp}^y.

Thermal noise in the normal-metal layer activates a fluctuating spin current flowing from the normal metal to the ferromagnet [44],

$$\mathbf{I}_{fl}(t) = -\frac{M_s V}{\gamma}\mathbf{m}(t) \times \boldsymbol{\zeta}'(t). \tag{2}$$

Here, V is the total volume of the ferromagnet, γ is the gyromagnetic factor, and $\boldsymbol{\zeta}'(t) = \gamma \mathbf{h}'(t)$ with $\mathbf{h}'(t)$ denoting the random magnetic field. In the classical limit $k_B T \gg \hbar\omega_0$, the correlation function $\langle \zeta_i'(t)\zeta_j'(t')\rangle$ of $\boldsymbol{\zeta}'(t)$ reads

$$\langle \zeta_i'(t)\zeta_j'(t')\rangle = \frac{2\alpha'\gamma k_B T_N}{M_s V}\delta_{ij}\delta(t) \equiv \sigma'^2\delta_{ij}\delta(t), \tag{3}$$

where $\langle \cdots \rangle$ denotes the ensemble average and $i, j = x, y, z$. Furthermore, ω_0 is the ferromagnetic resonance frequency, and α' is the contribution to the damping constant due to spin pumping $\alpha' = \gamma\hbar g_r/4\pi M_s V$. We emphasize that the correlator [Eq. (3)] is proportional to the temperature T_N.

The total spin current flowing through the ferromagnet/normal-metal interface is given by the sum of pumping and fluctuating spin currents $\mathbf{I}_{\rm tot} = \mathbf{I}_{sp} + \mathbf{I}_{fl}$. For clarity of notation, we omit here (and in the following) the time dependence of spin currents, normalized magnetization, random magnetic fields, and their correlators. This dependence will be restored if necessary. According to Eqs. (1) and (2), the total average spin current flowing across the interface can be written in the following form [43]:

$$\langle \mathbf{I}_{\rm tot}\rangle = \frac{M_s V}{\gamma}[\alpha'\langle \mathbf{m}\times\dot{\mathbf{m}}\rangle - \langle \mathbf{m}\times\boldsymbol{\zeta}'\rangle]. \tag{4}$$

Now, we assume that a spatially uniform current of density $\mathbf{j}_a = j_a\mathbf{i}_x$ is injected along the x axis. This current gives rise to additional torques owing to the spin-Hall effect and Rashba spin-orbit interaction. Thus, the magnetization dynamics is then modified and is governed by the stochastic LLG equation [27],

$$\frac{d\mathbf{m}}{dt} = -\gamma\mathbf{m}\times(\mathbf{H}_{\rm eff}+\mathbf{h}) + \alpha\mathbf{m}\times\dot{\mathbf{m}} + \boldsymbol{\tau}_{SO}, \tag{5}$$

where α is the Gilbert damping constant, $\mathbf{h}$ is the time-dependent random magnetic field in the ferromagnet, and $\mathbf{H}_{\rm eff}$ is an effective field. This effective field consists of three contributions: the exchange field, the external magnetic field oriented along the y axis, and the field corresponding to the DM interaction,

$$\begin{aligned}\mathbf{H}_{\rm eff} &= \frac{2A}{\mu_0 M_s}\nabla^2\mathbf{m} + H_0\mathbf{y} - \frac{1}{\mu_0 M_s}\frac{\delta E_{DM}}{\delta\mathbf{m}},\\ E_{DM} &= D[m_z\nabla\mathbf{m} - (\mathbf{m}\nabla)m_z].\end{aligned} \tag{6}$$

For the sake of simplicity, in the analytical part, we take into account only the external magnetic field. In turn, the term $\boldsymbol{\tau}_{SO}$ in Eq. (5) describes SO torques related to the Rashba SO coupling and the spin-Hall effect,

$$\begin{aligned}\boldsymbol{\tau}_{SO} = &-\gamma\mathbf{m}\times\mathbf{H}_R + \gamma\eta\xi\mathbf{m}\times(\mathbf{m}\times\mathbf{H}_R)\\ &+\gamma\mathbf{m}\times(\mathbf{m}\times\mathbf{H}_{SH}),\end{aligned} \tag{7}$$

where ξ is a nonadiabatic parameter and $\eta = 1$ when the torque has a Slonczewski-like form, whereas $\eta = 0$ in the opposite case [27]. In the above equation, the DM interaction enters the effective magnetic field, whereas the effect of Rashba SO coupling and spin-Hall effect are included by means of the extra torque added to the LLG equation.

As already mentioned above, the charge current flowing in the thin ferromagnetic layer leads to spin polarization at the ferromagnet/oxide interface. The accumulated spin density in the vicinity of the interface interacts with the local magnetization by means of the exchange coupling. This effect may be described by an effective Rashba field $\mathbf{H}_R = H_R\mathbf{i}_y$ [5,24,31],

$$\mathbf{H}_R = \frac{\alpha_R P}{\mu_0\mu_B M_s}(\mathbf{i}_z\times\mathbf{j}_a) = \frac{\alpha_R P j_a}{\mu_0\mu_B M_s}\mathbf{i}_y, \tag{8}$$

where α_R is the Rashba parameter and P is the degree of spin polarization of conduction electrons [31]. The first term in Eq. (7) corresponds to the out-of-plane torque and is related to the effective field H_R. This torque is oriented perpendicularly to the $(\mathbf{m}, \mathbf{H}_R)$ plane. The second term in Eq. (7) captures the effects of spin diffusion inside the magnetic layer and the spin current associated with the Rashba interaction at the interface. For more details, we refer to Ref. [24].

The last term in Eq. (7) corresponds to the spin-Hall torque [32,33], expressed by the spin-Hall field $\mathbf{H}_{SH}$. The spin current is generated due to the spin-Hall effect in the heavy-metal layer and is injected into the ferromagnetic layer. For more details, we refer to Refs. [34–36]. The explicit expression for $\mathbf{H}_{SH}$ reads

$$\mathbf{H}_{SH} = \frac{\hbar\theta_{SH} j_a}{\mu_0 2e M_s L_z}\mathbf{i}_y, \tag{9}$$

where L_z is the thickness of the ferromagnetic layer, whereas θ_{SH} is the spin-Hall angle (defined as the ratio of spin current and charge current densities).

As already mentioned above, total random magnetic-field $\mathbf{h}(t)$ has two contributions from different noise sources: the thermal random field $\mathbf{h}_0(t)$ and the random field $\mathbf{h}'(t)$. Since the random fields are statistically independent, their correlators are additive and fully determined by the total (enhanced) magnetic damping $\alpha = \alpha_0 + \alpha'$ [43] (with α_0 being the damping parameter of the ferromagnetic material, i.e., without contributions from pumping currents),

$$\langle\zeta_i(t)\zeta_j(0)\rangle = \frac{2\alpha\gamma k_B T_F^m}{M_s V}\delta_{ij}\delta(t) = \sigma^2\delta_{ij}\delta(t), \tag{10}$$

where $\boldsymbol{\zeta}(t) = \gamma\mathbf{h}(t)$ and $\alpha T_F^m = \alpha_0 T_F + \alpha' T_N$.

III. SPIN CURRENT: N/F STRUCTURE

The injected electrical current creates a transverse spin current in the heavy-metal layer via the spin-Hall effect (or spin accumulation at the boundaries of the sample) [41]. In turn, the Rashba SO interaction in the presence of charge current gives rise to additional torque as already described above. In the case under consideration, the Rashba SO field, Eq. (8), and the spin-Hall field, Eq. (9), are oriented along the y axis. When temperature of the ferromagnetic film differs from that of the normal-metal $T_F \neq T_N$, the spin-Seebeck current emerges in the Fe/N contact. Note, this current also exists in the absence of spin-orbit interaction and for $j_a = 0$. Below, we calculate the total spin current in the N/F structure, taking into account the Rashba SO field and the spin-Hall effect.

In order to calculate the spin pumping current $\langle\mathbf{I}_{sp}\rangle = \frac{M_s V}{\gamma}\alpha'\langle\mathbf{m}\times\dot{\mathbf{m}}\rangle$, we use Eq. (A1) (see Appendix A) and find

$$\langle\mathbf{I}_{sp}\rangle = \alpha'\frac{M_s V}{\gamma}(-\langle\mathbf{m}\times\boldsymbol{\omega}_2\rangle - \langle\mathbf{m}\times\mathbf{m}\times\boldsymbol{\omega}_1\rangle), \tag{11}$$

where $\boldsymbol{\omega}_1$ and $\boldsymbol{\omega}_2$ are defined in Appendix A, see Eq. (A1). Utilizing Eqs. (A2) and (A15), we find mean values of the magnetization components (see Appendix B),

$$\begin{aligned}\langle m_y\rangle &= -L(\beta\omega_2), \quad \langle m_y^2\rangle = 1 - \frac{2L(\beta\omega_2)}{\beta\omega_2},\\ \langle m_x^2\rangle &= \langle m_z^2\rangle = \frac{L(\beta\omega_2)}{\beta\omega_2},\end{aligned} \tag{12}$$

where $\beta = 2/\sigma^2$ and $L(x) = \coth x - \frac{1}{x}$ is the Langevin function. From Eq. (12) we obtain $\langle\mathbf{m}\times\boldsymbol{\omega}_2\rangle = 0$ and $\langle(\mathbf{m}\times\dot{\mathbf{m}})_x\rangle = 0$, $\langle(\mathbf{m}\times\dot{\mathbf{m}})_y\rangle = -\omega_1(1 - \langle m_y^2\rangle)$, $\langle(\mathbf{m}\times\dot{\mathbf{m}})_z\rangle = 0$. Thus, the only nonzero component of the spin pumping

current is,

$$\langle \mathbf{I}^y_{sp} \rangle = \alpha' \frac{M_s V}{\gamma} \omega_1 \left(1 - \langle m_y^2 \rangle\right) = \alpha' \frac{M_s V}{\gamma} \frac{2\omega_1}{\beta\omega_2} L(\beta\omega_2). \tag{13}$$

For the evaluation of the fluctuating spin current $\langle \mathbf{I}_{\mathbf{fl}} \rangle = -\frac{M_s V}{\gamma} \langle \mathbf{m} \times \zeta' \rangle$, we linearize the LLG equation, Eq. (A1), near the equilibrium point $\langle m_x \rangle = \langle m_z \rangle = 0$, $\langle m_y \rangle = -L(\beta\omega_2)$,

$$\dot{m}_x = \omega_1 m_z + \omega_2 \langle m_y \rangle m_x - \langle m_y \rangle \zeta_z(t),$$
$$\dot{m}_z = -\omega_1 m_z + \omega_2 \langle m_y \rangle m_z + \langle m_y \rangle \zeta_x(t). \tag{14}$$

Fourier transforming to the frequency domain ($\tilde{g} = \int g e^{i\omega t} dt$ and $g = \int \tilde{g} e^{-i\omega t} d\omega/2\pi$) from Eq.(14) we obtain $\tilde{m}_i(\omega) = \sum_j \chi_{ij}(\omega) \tilde{\zeta}_j(\omega)$, where $i, j = x, z$ and

$$\chi_{ij}(\omega) = \frac{\langle m_y \rangle}{(\omega_2 \langle m_y \rangle + i\omega)^2 + \omega_1^2} \times \begin{pmatrix} \omega_1 & (\omega_2 \langle m_y \rangle + i\omega) \\ -(\omega_2 \langle m_y \rangle + i\omega) & \omega_1 \end{pmatrix}, \tag{15}$$

$$\langle m_i(t) \zeta'_x(0) \rangle = \sigma'^2 \int_{-\infty}^{+\infty} \chi_{ij}(\omega) e^{-i\omega t} \frac{d\omega}{2\pi}. \tag{16}$$

Equation (16) has nonzero elements,

$$\langle m_z(t) \zeta'_x(0) \rangle = -\langle m_x(t) \zeta'_z(0) \rangle = -\sigma'^2 \langle m_y \rangle \int_{\infty}^{+\infty} \frac{\omega_2 \langle m_y \rangle + i\omega}{(\omega_2 \langle m_y \rangle + i\omega)^2 + \omega_1^2} e^{-i\omega t} \frac{d\omega}{2\pi}. \tag{17}$$

Details of calculating the integral in Eq. (17) are presented in Appendix C. Taking into account Eq. (17) one obtains

$$\langle \mathbf{m} \times \boldsymbol{\zeta}' \rangle_y = \langle m_z \zeta'_x - m_x \zeta'_z \rangle = -\sigma'^2 L(\beta\omega_2). \tag{18}$$

The fluctuating spin current has only one nonzero component, i.e., the y component—similarly as the spin pumping current does

$$\langle \mathbf{I}^y_{fl} \rangle = \frac{M_s V}{\gamma} \sigma'^2 L(\beta\omega_2). \tag{19}$$

We emphasize that, when calculating the spin pumping current, we did not employ a linearization procedure. Accordingly, the expression for the spin pumping current, Eq. (13), is valid for an arbitrary deviation of the magnetization from the ground-state magnetic order, even for thermally assisted magnetization-reversal instability processes, meaning the transversal components m_x, m_y can be arbitrarily large. On the other hand, the expression for the fluctuation spin current, Eq. (19), was obtained upon a linearization near the equilibrium point as described at the beginning of this paragraph. Taking into account the above derived formula Eqs. (13) and (19) for spin pumping and fluctuation currents, respectively, we deduce the following expression of the total spin current:

$$\langle \mathbf{I}^y_{\text{tot}} \rangle = \frac{M_s V}{\gamma} L(\beta\omega_2) \left[\alpha' \frac{\sigma^2 \omega_1}{\omega_2} + \sigma'^2 \right]. \tag{20}$$

When $\mathbf{H}_{\text{eff}} = (0, H_0, 0)$, where H_0 is the external magnetic field oriented along the y axis [5], then using Eqs. (3), (10), and (A2), one obtains from Eq. (20),

$$\langle I^y_{\text{tot}} \rangle = 2\alpha' k_B L \left(\frac{M_s V(\alpha H_0 + (\alpha - \eta\xi) H_R - H_{SH})}{\alpha k_B T_F^m} \right) \times \left(\frac{\alpha(H_0 + H_R + \alpha H_{SH}) T_F^m}{\alpha H_0 + (\alpha - \eta\xi) H_R - H_{SH}} - T_N \right), \tag{21}$$

where $\eta = 0, 1$ and we inspect, in the following, the $\eta = 0$ case.

We analyze now in more detail Eq. (21) for $\eta = 0$ and for several asymptotic cases. Let us begin with the case of a negligible spin-Hall effect. Assuming a small H_{SH}, $H_{SH} \ll \alpha H_R, \alpha H_0$, we derive from Eq. (21) the spin current in the following two regimes: (i) The low-temperature regime $M_s V(H_0 + H_R)/k_B T_F^m \gg 1$, and (ii) the high-temperature regime $M_s V(H_0 + H_R)/k_B T_F^m \ll 1$. These two regimes can be equivalently referred to as the high and weak magnetic-field limits, respectively. In particular, in the low-temperature limit, upon taking into account the property of the Langevin function $L(x) = \coth(x) - 1/x$, $L(x \gg 1) \approx 1$, we find that the spin current depends neither on the SO coupling nor on the external magnetic-field $\langle I^y_{\text{tot}} \rangle = 2\alpha' k_B (T_F^m - T_N)$ and is solely determined by the temperature bias. In the low-temperature regime (strong magnetic field), the magnetic fluctuations are small, and the spin current is then linear in the averaged square of these fluctuations. The latter, in turn, are linear in the relevant temperature. Accordingly, the spin current is proportional to the temperature bias. In the high-temperature limit (or equivalently a small magnetic field), the magnetic fluctuations are relatively large. Taking into account the asymptotic limit of the Langevin function $L(x \ll 1) \approx x/3$, the spin current in the high magnon temperature limit is $\langle I^y_{\text{tot}} \rangle = (2/3)\alpha' M_s V(H_0 + H_R)(T_F^m - T_N)/T_F^m$. Thus, the spin current is reduced by the factor of $(H_0 + H_R)/T_F^m$, which decreases with increasing magnon temperature or decreasing magnetic field. Note, the spin current is enhanced when the Rashba and the external fields are parallel and is reduced in the antiparallel case. Remarkably, the saturation of the spin current is observed in the high magnon temperature limit $T_F^m \gg T_N$, where $\langle I^y_{\text{tot}} \rangle \approx (2/3)\alpha' M_s V(H_0 + H_R)$.

Let us assume now a sizable spin-Hall field that cannot be neglected. The first specific case is when $H_{SH} \approx \alpha(H_0 + H_R)$. Taking into account the asymptotic limit of the Langevin function $L(x \ll 1) \approx x/3$ in the high magnon temperature limit $M_s V(\alpha H_0 + \alpha H_R - H_{SH})/\alpha k_B T_F^m \ll 1$, one finds the following expression for the spin current:

$$\langle I^y_{\text{tot}} \rangle = \frac{2}{3} \alpha' M_s V \left[(H_0 + H_R + \alpha H_{SH}) - \frac{T_N}{T_F^m} \frac{(\alpha H_0 + \alpha H_R - H_{SH})}{\alpha} \right]. \tag{22}$$

Since $\alpha(H_0 + H_R) \approx H_{SH}$, the second term for any finite T_N/T_F^m in Eq. (22) is small and can be neglected. Thus, the saturated spin current is

$$\langle I^y_{\text{tot}} \rangle = \frac{2}{3} \alpha' M_s V(H_0 + H_R + \alpha H_{SH}). \tag{23}$$

The expression for the saturated spin current, Eq. (23), does not depend on the temperature. However, Eq. (23) is valid only if the magnon temperature T_F^m is high enough. Thus, by tuning the applied external magnetic-field H_0, a nonzero spin pumping current can be achieved at arbitrary and even at equal temperatures $T_F^m = T_N$. For the opposite external and Rashba fields $H_0 = -H_R$ from Eq. (21) follows:

$$\langle I_{\rm tot}^y \rangle = 2\alpha' k_B L \left(\frac{M_s V H_{SH}}{\alpha k_B T_F^m} \right) (\alpha^2 T_F^m + T_N). \tag{24}$$

The obtained result is remarkable as it shows that the net pumping current is finite at arbitrary nonzero temperatures T_F^m and T_N in the absence of the applied temperature gradient.

Finally, we explore the case when the fields are comparable $H_{SH} \approx H_R \approx H_0$. Since $\alpha \ll 1$, then $H_{SH} \gg \alpha H_R, \alpha H_0$, and the total spin current

$$\langle I_{\rm tot}^y \rangle = 2\alpha' k_B L \left(\frac{M_s V (\alpha H_0 + \alpha H_R - H_{SH})}{\alpha k_B T_F^m} \right) \times \left\{ \frac{\alpha (H_0 + H_R + \alpha H_{SH}) T_F^m}{(\alpha H_0 + \alpha H_R - H_{SH})} - T_N \right\}.$$

in this case reads

$$\langle I_{\rm tot}^y \rangle = 2\alpha' k_B L \left(\frac{M_s V H_{SH}}{\alpha k_B T_F^m} \right) \left\{ \frac{\alpha (H_0 + H_R) T_F^m}{H_{SH}} + T_N \right\}. \tag{25}$$

In the low magnon temperature limit we deduce

$$\langle I_{\rm tot}^y \rangle = 2\alpha' k_B \left\{ \frac{\alpha (H_0 + H_R) T_F^m}{H_{SH}} + T_N \right\}, \tag{26}$$

while in the high magnon temperature limit one finds

$$\langle I_{\rm tot}^y \rangle = \frac{2}{3} M_s V \left\{ (H_0 + H_R) + \frac{H_{SH}}{\alpha} \frac{T_N}{T_m^F} \right\}. \tag{27}$$

As we see from Eqs. (26) and (27), the role of field H_{SH} is different. In the low magnon temperature limit, it reduces the spin pumping current, whereas in the high magnon temperature limit, it enhances the fluctuating spin current.

In the analytical calculation, we assumed that temperatures of the magnon subsystem and normal metal are fixed during the process. However, this is an approximation because the temperatures of the subsystems change slightly during the equilibration process. For illustration, we consider the case when the external and Rashba fields H_0 and H_R are parallel, and we neglect the spin-Hall term. Then, from Eq. (21) we deduce

$$\langle I_{\rm tot}^y \rangle = 2\alpha' k_B L \left(\frac{M_s V (H_0 + H_R)}{k_B T_F^m} \right) (T_F^m - T_N). \tag{28}$$

Apparently the total spin current is zero when $T_F^m = T_N$. However, the magnon temperature T_F^m that we used for derivation of the Fokker-Planck equation is the initial magnon temperature. The electric current due to the Rashba field modifies the magnon density and magnon temperature, leading to a slight difference in effective magnon temperatures $T_F^m(j_a) - T_F^m(j_a = 0) = \delta T_F^m$. This correction is beyond the Fokker-Planck equation. Therefore, due to the temperature correction δT_F^m, in the numerical calculations we expect to obtain a finite net current even when the initial magnon temperature is equal to the temperature of the normal metal $T_F^m(j_a = 0) = T_N$.

IV. SPIN CURRENT IN THE $N/F/N$ STRUCTURE

The same method has been utilized to calculate the spin current in the $N/F/N$ system shown schematically in Fig. 2. We calculate the spin current defined as the difference in spin currents flowing through the two interfaces,

$$\mathbf{I}_{\rm tot} = \mathbf{I}_{\rm tot1} - \mathbf{I}_{\rm tot2}$$
$$\mathbf{I}_{\rm tot1} = \mathbf{I}_{fl1} + \mathbf{I}_{sp1}, \quad \mathbf{I}_{\rm tot2} = \mathbf{I}_{fl2} + \mathbf{I}_{sp2}. \tag{29}$$

Here, $\mathbf{I}_{\rm tot1}$ and $\mathbf{I}_{\rm tot2}$ are the total spin current in the first and second interfaces. The total spin current includes four terms. Two terms $\mathbf{I}_{sp1}$ and $\mathbf{I}_{sp2}$ describe the spin pumping currents from the ferromagnetic layer to the left N_1 metallic layer and to the right N_2 metallic layer, respectively. In turn, the terms $\mathbf{I}_{fl1}$ and $\mathbf{I}_{fl2}$ describe the fluctuating spin currents flowing from the left and right metallic layers towards the ferromagnetic layer. We assume that the two metals have different temperatures T_{N_1} and T_{N_2}. The spin pumping current flowing from the ferromagnetic layer towards metallic layers ($i = 1, 2$) reads

$$\langle I_{sp1}^y \rangle = \alpha'(T_{N_1}) \frac{M_s V}{\gamma} \frac{2\omega_1}{\beta\omega_2} L(\beta\omega_2),$$
$$\langle I_{sp2}^y \rangle = -\alpha'(T_{N_2}) \frac{M_s V}{\gamma} \frac{2\omega_1}{\beta\omega_2} L(\beta\omega_2). \tag{30}$$

In turn, the fluctuating currents have the components,

$$\langle I_{fl1}^y \rangle = 2\alpha'(T_{N_1}) k_B T_{N_1} L(\beta\omega_2),$$
$$\langle I_{fl2}^y \rangle = -2\alpha'(T_{N_2}) k_B T_{N_2} L(\beta\omega_2). \tag{31}$$

As we can see from Eqs. (30) and (31), the difference in the two components of the spin pumping current and the fluctuating current is related to the temperature dependence of the damping constant $\alpha'(T_N)$. For convenience, we denote $\alpha'(T_{N_1}) = \alpha'$ and $\alpha'(T_{N_2}) = \alpha' + \Delta\alpha$. If the difference between the temperatures of the metals T_{N_1} and T_{N_2} is not too large, the variation of the damping constant $\Delta\alpha'$ is very small $|\Delta\alpha'|/\alpha' \ll 1$ [48,49]. In such a case,

$$\langle I_{\rm tot1}^y \rangle = 2\alpha' k_B L(\beta\omega_2) \left(\alpha \frac{\omega_1}{\omega_2} T_F^m + T_{N_1} \right),$$
$$\langle I_{\rm tot2}^y \rangle = -2\alpha' k_B L(\beta\omega_2) \left(\alpha \frac{\omega_1}{\omega_2} T_F^m + T_{N_2} \right), \tag{32}$$

and total spin current,

$$\langle I_{\rm tot}^y \rangle = 2\alpha' k_B L(\beta\omega_2) \left(2\alpha \frac{\omega_1}{\omega_2} T_F^m + T_{N_1} + T_{N_2} \right). \tag{33}$$

When $\mathbf{H}_{\rm eff} = (0, H_0, 0)$, then using Eqs.(3),(10), and (A2), one obtains from Eq. (33),

$$\langle I_{\rm tot}^y \rangle = 2\alpha' k_B L \left(\frac{M_s V (\alpha H_0 + (\alpha - \eta\xi) H_R - H_{SH})}{\alpha k_B T_F^m} \right) \times \left(2 \frac{\alpha (H_0 + H_R + \alpha H_{SH}) T_F^m}{\alpha H_0 + (\alpha - \eta\xi) H_R - H_{SH}} - T_{N_1} - T_{N_2} \right). \tag{34}$$

When $\eta = 0$ and $H_{SH} \ll \alpha H_0, \alpha H_R$ from Eq. (34) we get

$$\langle I^y_{\rm tot}\rangle = 2\alpha' k_B L\left(\frac{M_s V(H_0+H_R)}{k_B T_F^m}\right)\left(2T_F^m - T_{N_1} - T_{N_2}\right). \tag{35}$$

Again we see that the larger the difference between magnon and metal temperatures, the larger the total spin current.

V. EFFECT OF DM INTERACTION

In order to explore the role of DM interaction, we performed micromagnetic simulations for a finite-size N/F system. To be more specific, we study Pt/Co/AlO where the Co layer is 500 nm × 50 nm large with a thickness of 10 nm. The Co layer is sandwiched between Pt and AlO films. The following parameters describe the Co layer: the saturation magnetization of $M_s = 10^6$ A/m, and the damping constant $\alpha = 0.2$. The Rashba field $H_R = \frac{\alpha_R P}{\mu_B \mu_0 M_s} j_a$ can be estimated assuming $P = 0.5$, $\alpha_R = 10^{-10}$ eV m, and the spatially uniform current density j_a along the x axis on the order of 10^{12} A/m^2. Due to the structure of the Rashba field, an increase in the magnitude of current density j_a is formally equivalent to the corresponding increase in the SO constant α_R. Thus, the dependence of the total spin current on the current density j_a is equivalent to the dependence of the total spin current on the SO constant α_R.

In Fig. 3, the total spin current $I^y_{\rm tot} = \langle I^y_{\rm tot}\rangle$ is plotted as a function of the electric current density j_a (assumed negative) for the case when the external magnetic field H_0 and the Rashba field H_R are parallel. When $j_a = 0$, the total spin current is solely the spin-Seebeck current and is absent for equal temperatures $T_F^m(j_a = 0) = T_N$. However, when $|j_a| > 0$, the total spin current is nonzero as well. As it was already mentioned above, the reason of a nonzero net spin current is a slight shift of the magnon temperature $T_F^m(|j_a| > 0) - T_F^m(j_a = 0) = \delta T_F^m$ and of the magnon density, that occur due to the charge current j_a. Apparently, in the case of antiparallel Rashba H_R and external H_0 magnetic fields, the total net spin current decreases with increasing magnitude of the charge current. This numerical result is consistent with the analytical results obtained in the previous section. As we see, the effect of the DM interaction is diverse: When $\delta T_F^m > 0$ and the spin current is positive $\langle I^y_{\rm tot}\rangle = \langle I^y_{sp}\rangle + \langle I^y_{fl}\rangle > 0$, $\langle I^y_{fl}\rangle < 0$ (i.e., the ferromagnetic layer is *hotter* than the normal-metal layer), the DM interaction enhances the current. However, in the case of $\delta T_F^m < 0$, when fluctuating spin current is larger than the spin pumping current and the total net current is negative $\langle I^y_{\rm tot}\rangle < 0$, the DM interaction reduces the spin current. This means that the Rashba H_R field always has a positive contribution to the spin pumping current. The situation is the same when the spin-Hall effect is included, see Fig. 4. As one can see, the spin-Hall effect has the opposite effect; it always decreases the spin pumping current. Therefore, for $\delta T_F^m > 0$,

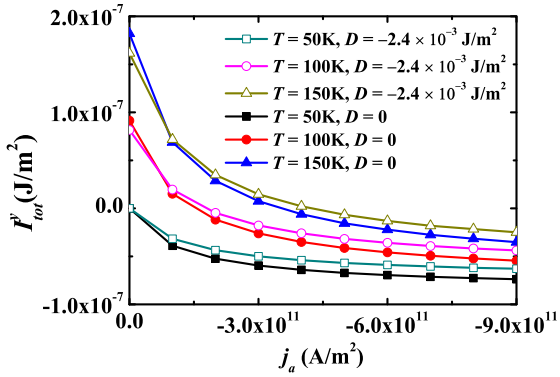

FIG. 3. Total spin current $I^y_{\rm tot}$ in the absence of the spin-Hall effect ($\theta_{SH} = 0$), plotted as a function of the electric current density j_a. The external field H_0 and the Rashba field H_R are parallel. The magnon temperature is $T \equiv T_F^m = 50$ K (squares), 100 K (circles), and 150 K (triangles). The DMI constant is assumed to be $D = 0$ (solid dots) and $D = -2.4 \times 10^{-3}$ J/m^2 (open dots). The external magnetic-field $H_0 = 4 \times 10^5$ A/m and the normal-metal temperature $T_N = 50$ K are assumed.

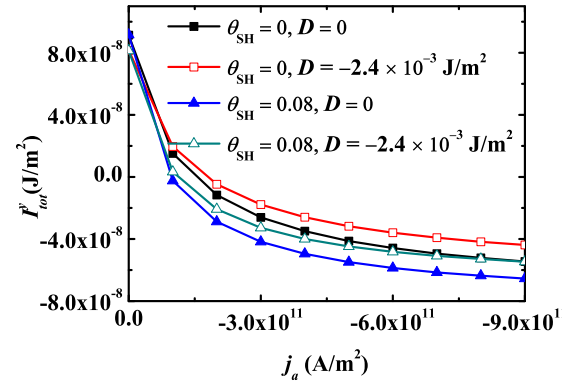

FIG. 4. The total spin current $I^y_{\rm tot}$ without the contribution of the spin-Hall effect ($\theta_{SH} = 0$, squares and with the spin-Hall effect ($\theta_{SH} = 0.08$, triangles), plotted as a function of the electric current density j_a. The external field H_0 and the Rashba field H_R are parallel. The DM interaction constant is assumed to be $D = 0$ (solid dots) and $D = -2.4 \times 10^{-3}$ J/m^2 (open dots). The external magnetic-field $H_0 = 4 \times 10^5$ A/m, the magnon temperature $T_F^m = 100$ K, and the normal-metal temperature $T_N = 50$ K are assumed.

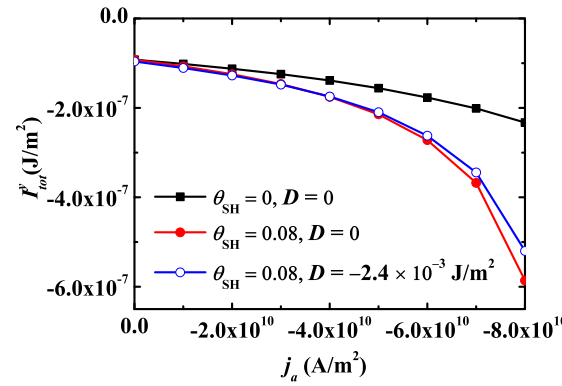

FIG. 5. The total spin current $I^y_{\rm tot}$ with the spin-Hall effect ($\theta_{SH} = 0.08$, circles) and without the spin-Hall effect ($\theta_{SH} = 0$, squares), plotted as a function of the electric current density j_a. The external field H_0 and the Rashba field H_R are antiparallel. The DMI constant is assumed to be $D = 0$ (solid dots) and $D = -2.4 \times 10^{-3}$ J/m^2 (open dots). The external magnetic field is $H_0 = -9 \times 10^5$ A/m, the magnon temperature is $T_F = 100$ K, and the temperature of normal metal is $T_N = 50$ K.

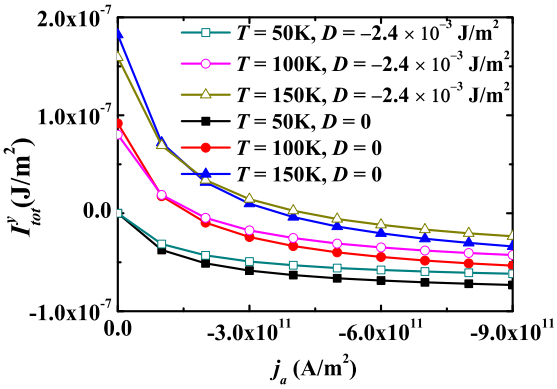

FIG. 6. Total spin current $I^y_{\rm tot}$ in the absence of spin-Hall contribution ($\theta_{SH} = 0$), plotted as a function of the electric current density j_a. The local magnetization and the Rashba field are parallel. The magnon temperature is $T \equiv T_F^m = 50$ K (squares), 100 K (circles), and 150 K (triangles). The DMI constant $D = 0$ (solid dots) and $D = -2.4 \times 10^{-3}$ J/m^2 (open dots). The magnetocrystalline anisotropy constant $K_y = 3 \times 10^5$ J/m^3 and the normal-metal temperature $T_N = 50$ K. The effective anisotropy field is $\mathbf{H}_{\rm ani} = 2K_y m_y \mathbf{e}_y/(\mu_0 M_s)$.

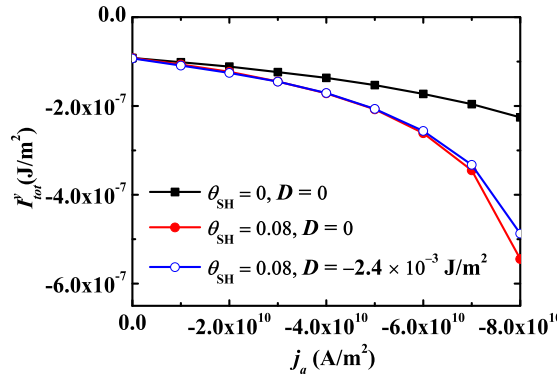

FIG. 8. The total spin current $I^y_{\rm tot}$ with the spin-Hall effect ($\theta_{SH} = 0.08$, circles) and without the spin-Hall effect ($\theta_{SH} = 0$, squares), plotted as a function of the electric current density j_a. The local magnetization and the Rashba field are antiparallel. DMI constant $D = 0$ (solid dots) and $D = -2.4 \times 10^{-3}$ J/m^2 (open dots). The external magnetic-field $H_0 = -5 \times 10^5$ A/m, the magnetocrystalline anisotropy constant $K_y = 3 \times 10^5$ J/m^3, the magnon temperature $T_F^m = 100$ K, and the normal-metal temperature $T_N = 50$ K. The effective anisotropy field is $\mathbf{H}_{\rm ani} = 2K_y m_y \mathbf{e}_y/(\mu_0 M_s)$.

the total spin current without the spin-Hall effect is larger, whereas for $\delta T_F^m < 0$, it is smaller.

Finally, we consider the case when the Rashba field H_R and the external magnetic H_0 field are parallel, see Fig. 4. Note that a switching of the direction of the magnetic field alters the ground-state magnetic order. Therefore, the spin current changes sign. As we see from Fig. 5, the spin current increases with the electric current density $|j_a|$. This result is also consistent with the analytical result obtained in the previous section.

In order to see the effect of magnetocrystalline anisotropy, we repeated the calculations with the anisotropy term being included. Results of the calculations, plotted in Figs. 6–8 show that the magnetocrystalline anisotropy has no significant

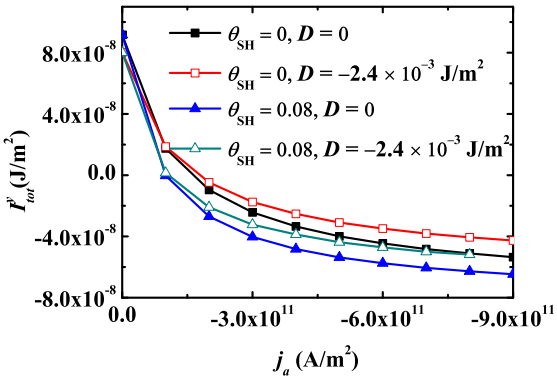

FIG. 7. Total spin current $I^y_{\rm tot}$ in the absence of the spin-Hall effect ($\theta_{SH} = 0$, squares) and with the Hall effect ($\theta_{SH} = 0.08$, triangles), plotted as a function of the electric current density j_a for the case when the local magnetization and the Rashba field are parallel. The DM interaction constant $D = 0$ (solid dots) and $D = -2.4 \times 10^{-3}$ J/m^2 (open dots). The magnetocrystalline anisotropy constant $K_y = 3 \times 10^5$ J/m^3, the magnon temperature $T_F^m = 100$ K, and the normal-metal temperature $T_N = 50$ K. The effective anisotropy field is $\mathbf{H}_{\rm ani} = 2K_y m_y \mathbf{e}_y/(\mu_0 M_s)$.

influence on the spin current, so the effects discussed above hold in the presence of the anisotropy as well.

VI. CONCLUSIONS

In this paper, we have considered two different heterostructures consisting of a thin ferromagnetic film sandwiched between heavy-metal and oxide layers. Interfacing the ferromagnetic layer to the heavy metal may result in spin-Hall torque exerted on the magnetic moment, whereas at the interface of the oxide material a spin-orbit coupling of the Rashba type emerges. Both factors (the spin-Hall effect and the Rashba spin-orbit coupling) have a significant influence on the magnetic dynamics and thus on the spin pumping current. The total spin current crossing the ferromagnetic/normal-metal interface has two contributions: the spin current pumped from the ferromagnetic metal to the normal one and the spin fluctuating current flowing in the opposite direction. The spin-Hall effect and the Rashba spin-orbit coupling influence only the spin pumping current and, therefore, impact the total spin current. We explored the spin-Seebeck current beyond the linear-response regime and found the following interesting features: If the external magnetic-field H_0 is parallel to the Rashba SO field H_R, then the SO coupling enhances the spin current, in the case of an antiparallel magnetic-field H_0 and a Rashba SO field H_R, the SO coupling decreases the spin current. The spin-Hall effect and the DM interaction always increase the spin pumping current. The results are confirmed analytically by means of the Fokker-Planck equation and by direct micromagnetic numerical calculations for a specific sample.

ACKNOWLEDGMENTS

This work is supported by the DFG through the SFB 762 and SFB-TRR 227, by the National Science Center in Poland as a research Project No. DEC-2017/27/B/ST3/02881, the National Natural Science Foundation of China No. 11704415,

and the Natural Science Foundation of Hunan Province of China No. 2018JJ3629.

APPENDIX A: DERIVATION OF THE FOKKER-PLANK EQUATION

For the derivation of the Fokker-Plank equation, we follow Ref. [50] and use the functional integration method in order to average the dynamics over all possible realizations of the random noise field. First, we rewrite the LLG equation [Eq. (5)] in the form

$$\frac{d\mathbf{m}}{dt} = -\mathbf{m}\times[\omega_1+\zeta(t)] + \mathbf{m}\times\mathbf{m}\times\boldsymbol{\omega}_2, \tag{A1}$$

where

$$\begin{aligned}\boldsymbol{\omega}_1 &= \boldsymbol{\omega}_{\text{eff}} + \boldsymbol{\omega}_R + \alpha\boldsymbol{\omega}_{SH},\\ \boldsymbol{\omega}_2 &= -\alpha\boldsymbol{\omega}_{\text{eff}} - \alpha\boldsymbol{\omega}_R + \eta\xi\boldsymbol{\omega}_R + \boldsymbol{\omega}_{SH},\\ \boldsymbol{\omega}_{\text{eff}} &= \gamma\mathbf{H}_{\text{eff}}, \quad \boldsymbol{\omega}_R = \gamma\mathbf{H}_R, \quad \boldsymbol{\omega}_{SH} = \gamma\mathbf{H}_{SH},\end{aligned} \tag{A2}$$

and $\gamma \to \gamma/(1+\alpha^2)$. Here, $\boldsymbol{\zeta}(t)$ is a random Langevin field with the following correlation properties:

$$\langle\boldsymbol{\zeta}(\mathbf{t})\rangle = 0, \tag{A3}$$

$$\langle\zeta_i(t)\zeta_j(t')\rangle = \sigma^2\delta_{ij}\delta(t-t'). \tag{A4}$$

We introduce the probability distribution function of the random Gaussian noise $\boldsymbol{\zeta}$,

$$F[\boldsymbol{\zeta}(\mathbf{t})] = \frac{1}{Z_\zeta}\exp\left[-\frac{1}{\sigma^2}\int_{-\infty}^{+\infty} d\tau\,\zeta^2(\tau)\right], \tag{A5}$$

where $Z_\zeta = \int D\boldsymbol{\zeta}\, F$ is the noise partition function. With the help of Eq. (A5), the average of any noise functional $A_{\boldsymbol{\zeta}}$ can be written as

$$\langle A[\boldsymbol{\zeta}]\rangle_\zeta = \int D\boldsymbol{\zeta}\, A[\boldsymbol{\zeta}]F[\boldsymbol{\zeta}]. \tag{A6}$$

Considering the obvious identity,

$$\frac{\delta\zeta_\alpha\tau}{\delta\zeta_\beta(t)} = \delta_{\alpha\beta}\delta(\tau-t), \tag{A7}$$

we can calculate first and second variations of $F[\boldsymbol{\zeta}(t)]$,

$$\frac{\delta F[\boldsymbol{\zeta}]}{\delta\zeta_\alpha(t)} = -\frac{1}{\sigma^2}\zeta_\alpha(t)F[\zeta], \tag{A8}$$

$$\frac{\delta^2 F[\boldsymbol{\zeta}]}{\delta\zeta_\alpha(t)\delta\zeta_\beta(t')} = \left[\frac{1}{\sigma^4}\zeta_\alpha(t)\zeta_\beta(t') - \frac{1}{\sigma^2}\delta_{\alpha\beta}\delta(t-t')\right]F[\boldsymbol{\zeta}]. \tag{A9}$$

For arbitrary n, we have

$$\int D\boldsymbol{\zeta}\,\frac{\delta^n F[\boldsymbol{\zeta}]}{\delta\zeta_{\alpha_1}(t_1)\delta\zeta_{\alpha_2}(t_2)\cdots\delta\zeta_{\alpha_n}(t_n)} = 0. \tag{A10}$$

Taking into account Eq. (A8) to Eq. (A10), we obtain (A3) and (A4). Now, we introduce the distribution function,

$$f(\mathbf{N},t) = \langle\boldsymbol{\pi}([\boldsymbol{\zeta}],t)\rangle_\zeta, \quad \boldsymbol{\pi}([\boldsymbol{\zeta}],t) = \delta[\mathbf{N}-\mathbf{m}(t)], \tag{A11}$$

on the sphere $|\mathbf{N}| = 1$. Taking into account the relation [50] $\dot{\boldsymbol{\pi}} = -\frac{\partial\boldsymbol{\pi}}{\partial\mathbf{N}}\dot{\mathbf{m}}(t)$ and the equation of motion, Eq. (A1), we deduce the Fokker-Plank equation,

$$\begin{aligned}\frac{\partial f}{\partial t} = \frac{\partial}{\partial\mathbf{N}}&[(\mathbf{N}\times\boldsymbol{\omega}_1) - (\mathbf{N}\times\mathbf{N}\times\boldsymbol{\omega}_2)\\ &+\mathbf{N}\times\langle\boldsymbol{\zeta}(t)\boldsymbol{\pi}([\boldsymbol{\zeta}],t)\rangle_\zeta].\end{aligned} \tag{A12}$$

To calculate $\langle\boldsymbol{\zeta}(t)\boldsymbol{\pi}([\boldsymbol{\zeta}],t)\rangle_\zeta$ we use the standard procedure, discussed, for example, in Ref. [50] and obtain

$$\langle\boldsymbol{\zeta}(t)\boldsymbol{\pi}([\boldsymbol{\zeta}],t)\rangle_\zeta = -\frac{\sigma^2}{2}\mathbf{N}\times\frac{\partial f}{\partial\mathbf{N}}. \tag{A13}$$

The Fokker-Plank equation in the final form reads

$$\frac{\partial f}{\partial t} = \frac{\partial}{\partial\mathbf{N}}\left[(\mathbf{N}\times\boldsymbol{\omega}_1) - (\mathbf{N}\times\mathbf{N}\times\boldsymbol{\omega}_2) - \frac{\sigma^2}{2}\mathbf{N}\times\frac{\partial f}{\partial\mathbf{N}}\right]. \tag{A14}$$

The stationary solution of the Fokker-Plank equation when $\boldsymbol{\omega_1} \parallel \boldsymbol{\omega_2}$ has the form

$$f(\mathbf{N}) = \frac{\exp\left(-\frac{2}{\sigma^2}\int d\mathbf{N}\cdot\boldsymbol{\omega_2}\right)}{\int d\mathbf{N}\,\exp\left(-\frac{2}{\sigma^2}\int d\mathbf{N}\cdot\boldsymbol{\omega_2}\right)}. \tag{A15}$$

APPENDIX B: MEAN VALUES OF MAGNETIZATION

Exploiting the parametrization,

$$\begin{aligned}&m_x = \sin\theta\,\cos\varphi, \quad m_y = \sin\theta\,\cos\varphi, \quad m_z = \cos\theta,\\ &0\leqslant\theta\leqslant\pi, \quad 0\leqslant\varphi\leqslant 2\pi,\end{aligned} \tag{B1}$$

and taking into account Eq. (A15) and the parametrization Eq. (B1), we can write the probability distribution for $\mathbf{m}$,

$$\begin{aligned}dw(\theta,\varphi) &= \frac{1}{Z}f(\theta,\varphi)d\mathbf{m},\\ f(\theta,\varphi) &= \exp(-\beta\omega_2\sin\theta\,\sin\varphi),\\ dm &= \sin\theta\,d\theta\,d\varphi, \quad \beta = \frac{2}{\sigma^2}.\end{aligned} \tag{B2}$$

Here $Z = \frac{4\pi\,\sin(\beta\omega_2)}{\beta\omega_2}$ is the partition function. From Eq. (B2) we can calculate the mean values of the magnetization,

$$\begin{aligned}&\langle m_x\rangle = \langle m_z\rangle = 0, \quad \langle m_y\rangle = -L(\beta\omega_2),\\ &\langle m_x^2\rangle = \langle m_z^2\rangle = \frac{L(\beta\omega_2)}{\beta\omega_2}, \quad \langle m_y^2\rangle = 1 - \frac{2L(\beta\omega_2)}{\beta\omega_2},\\ &\langle m_x m_y\rangle = \langle m_z m_y\rangle = 0.\end{aligned} \tag{B3}$$

APPENDIX C: DERIVATION OF EQ. (17)

To calculate (17) we utilize Jourdan's lemma,

$$\begin{aligned}&\int_{-\infty}^{+\infty}\frac{\omega_2\langle m_y\rangle + i\omega}{(\omega_2\langle m_y\rangle + i\omega)^2+\omega_1^2}e^{-i\omega t}\frac{d\omega}{2\pi}\\ &= \int_{-\infty}^{+\infty}\frac{\omega_2\langle m_y\rangle - i\omega}{(\omega_2\langle m_y\rangle - i\omega)^2+\omega_1^2}e^{i\omega t}\frac{d\omega}{2\pi}\\ &= \begin{cases}-\frac{1}{2}(e^{-i(\omega_1+i\omega_2\langle m_y\rangle)t} + e^{i(\omega_1-i\omega_2\langle m_y\rangle)t}), & \text{if } t>0,\\ 0, & \text{if } t<0.\end{cases}\end{aligned} \tag{C1}$$

This integral is discontinuous at $t=0$, therefore the value $\langle\mathbf{m}(t)\times\boldsymbol{\zeta}'(\mathbf{0})\rangle_y$ at $t=0$ is given by the average of the values at $t=0^{\pm}$. Therefore, from Eq. (C1) we deduce Eq. (18),

$$\langle\mathbf{m}(0)\times\boldsymbol{\zeta}'(0)\rangle_y = \sigma'^2\langle m_y\rangle = -\sigma'^2 L(\beta\omega_2).$$

[1] Y. A. Bychkov and E. I. Rasbha, Pis'ma v Zh. Eksp. Teor. Fiz. **39**, 66 (1984) [JETP Lett. **39**, 78 (1984)].

[2] C. L. Kane and E. J. Mele, Phys. Rev. Lett. **95**, 226801 (2005).

[3] Y. J. Lin, K. Jimenez-Garcia, and I. B. Spielman, Nature (London) **471**, 83 (2011).

[4] E. I. Rashba and A. L. Efros, Phys. Rev. Lett. **91**, 126405 (2003).

[5] I. M. Miron, T. Moore, H. Szambolics, L. D. Buda-Prejbeanu, S. Auffret, B. Rodmacq, S. Pizzini, J. Vogel, M. Bonfim, A. Schuhl, and G. Gaudin, Nature Mater. **10**, 419 (2011).

[6] P. P. J. Haazen, E. Mure, J. H. Franken, R. Lavrijsen, H. J. M. Swagten, and B. Koopmans, Nature Mater. **12**, 299 (2013).

[7] A. A. Kovalev, V. A. Zyuzin, and B. Li, Phys. Rev. B **95**, 165106 (2017).

[8] U. Ritzmann, D. Hinzke, and U. Nowak, Phys. Rev. B **95**, 054411 (2017).

[9] P. Yan, G. E. W. Bauer, and H. Zhang, Phys. Rev. B **95**, 024417 (2017).

[10] J. Barker and G. E. W. Bauer, Phys. Rev. Lett. **117**, 217201 (2016).

[11] K. I. Uchida, H. Adachi, T. Kikkawa, A. Kirihara, M. Ishida, S. Yorozu, S. Maekawa, and E. Saitoh, Proc. IEEE **104**, 1946 (2016).

[12] E.-J. Guo, J. Cramer, A. Kehlberger, C. A. Ferguson, D. A. MacLaren, G. Jakob, and M. Kläui, Phys. Rev. X **6**, 031012 (2016).

[13] M. Schreier, F. Kramer, H. Huebl, S. Geprägs, R. Gross, S. T. B. Goennenwein, T. Noack, T. Langner, A. A. Serga, B. Hillebrands, and V. I. Vasyuchka, Phys. Rev. B **93**, 224430 (2016).

[14] S. R. Boona, S. J. Watzman, and J. P. Heremans, APL Mater. **4**, 104502 (2016).

[15] V. Basso, E. Ferraro, and M. Piazzi, Phys. Rev. B **94**, 144422 (2016).

[16] G. Lefkidis and S. A. Reyes, Phys. Rev. B **94**, 144433 (2016).

[17] S. M. Rezende, A. Azevedo, and R. L. Rodriguez-Suarez, J. Phys. D: Appl. Phys. **51**, 174004 (2018).

[18] M. Bialek, S. Brechet, and J. P. Ansermet, J. Phys. D: Appl. Phys. **51**, 164001 (2018).

[19] J. M. Bartell, C. L. Jermain, S. V. Aradhya, J. T. Brangham, F. Yang, D. C. Ralph, and G. D. Fuchs, Phys. Rev. Appl. **7**, 044004 (2017).

[20] H. Yua, S. D. Brechetb, and J. P. Ansermet, Phys. Lett. A **381**, 825 (2017); L. Karwacki, J. Magn. Magn. Mater. **441**, 764 (2017).

[21] S. R. Etesami, L. Chotorlishvili, A. Sukhov, and J. Berakdar, Phys. Rev. B **90**, 014410 (2014); S. R. Etesami, L. Chotorlishvili, and J. Berakdar, Appl. Phys. Lett. **107**, 132402 (2015).

[22] L. Chotorlishvili, X.-G. Wang, Z. Toklikishvili, and J. Berakdar, Phys. Rev. B **97**, 144409 (2018).

[23] X.-G. Wang, L. Chotorlishvili, G.-H. Guo, A. Sukhov, V. Dugaev, J. Barnaś, and J. Berakdar, Phys. Rev. B **94**, 104410 (2016); X.-G. Wang, L. Chotorlishvili, G.-H. Guo, J. Berakdar, J. Phys. D: Appl. Phys. **50**, 495005 (2017); X.-G. Wang, L. Chotorlishvili, and J. Berakdar, Front. Mater. **4**, 19 (2017); X.-g. Wang, Z.-x. Li, Z.-w. Zhou, Y.-z. Nie, Q.-l. Xia, Z.-m. Zeng, L. Chotorlishvili, J. Berakdar, and G-h. Guo, Phys. Rev. B **95**, 020414(R) (2017).

[24] X. Wang and A. Manchon, Phys. Rev. Lett. **108**, 117201 (2012); A. Manchon and S. Zhang, Phys. Rev. B **79**, 094422 (2009).

[25] B. Gu, I. Sugai, T. Ziman, G. Y. Guo, N. Nagaosa, T. Seki, K. Takanashi, and S. Maekawa, Phys. Rev. Lett. **105**, 216401 (2010).

[26] L. Liu, T. Moriyama, D. C. Ralph, and R. A. Buhrman, Phys. Rev. Lett. **106**, 036601 (2011).

[27] E. Martinez, S. Emori, and G. S. D. Beach, Appl. Phys. Lett. **103**, 072406 (2013).

[28] K.-W. Kim, S.-M. Seo, J. Ryu, K.-J. Lee, and H.-W. Lee, Phys. Rev. B **85**, 180404(R) (2012).

[29] S. Emori, U. Bauer, S.-M. Ahn, E. Martinez, and G. S. D. Beach, Nature Mater. **12**, 611 (2013).

[30] R. Lavrijsen, P. P. Haazen, E. Mure, J. H. Franken, J. T. Kohlhepp, H. J. M. Swagten, and B. Koopmans, Appl. Phys. Lett. **100**, 262408 (2012).

[31] P. Gambardella and I. M. Miron, Philos. Trans. R. Soc., A **369**, 3175 (2011); I. M. Miron, G. Gaudin, S. Auffret, B. Rodmacq, A. Schuhl, S. Pizzini, J. Vogel, and P. Gambardella, Nature Mater. **9**, 230 (2010).

[32] M. I. D'yakonov and V. I. Perel, Pis'ma Zh. Eksp. Teor. Fiz. **13**, 657 (1971) [JETP Lett. **13**, 467 (1971)].

[33] J. E. Hirsch, Phys. Rev. Lett. **83**, 1834 (1999).

[34] L. Liu, C.-F. Pai, Y. Li, H. W. Tseng, D. C. Ralph, and R. A. Buhrman, Science **336**, 555 (2012).

[35] K. Kondou, H. Sukegawa, S. Mitani, K. Tsukagoshi, and S. Kasai, Appl. Phys. Express **5**, 073002 (2012).

[36] S.-M. Seo, K.-W. Kim, J. Ryu, H.-W. Lee, and K.-J. Lee, Appl. Phys. Lett. **101**, 022405 (2012).

[37] Z. Li and S. Zhang, Phys. Rev. B **69**, 134416 (2004).

[38] N. Okuma and K. Nomura, Phys. Rev. B **95**, 115403 (2017).

[39] F. Mahfouzi and N. Kioussis, Phys. Rev. B **95**, 184417 (2017).

[40] B. K. Nikolic, K. Dolui, M. D. Petrović, P. Plecháč, T. Markussen, and K. Stokbro, in *Handbook of Materials Modeling*, edited by W. Andreoni and S. Yip (Springer, Cham, Switzerland, 2018), Vol. 2, pp. 1–35.

[41] E. Saitoh and K. I. Uchida, in *Spin Seebeck Effect, Spin Current*, edited by S. Maekawa, S. O. Valenzuela, E. Saitoh, and T. Kimura (Oxford University Press, Oxford, 2012).

[42] K. I. Uchida, S. Takahashi, K. Harii, J. leda, W. Koshibee, K. Ando, S. Maekawa, and E. Saitoh, Nature (London) **455**, 778 (2008).

[43] J. Xiao, G. E. W. Bauer, K.-c. Uchida, E. Saitoh, and S. Maekawa, Phys. Rev. B **81**, 214418 (2010).

[44] J. Foros, A. Brataas, Y. Tserkovnyak, and G. E. W. Bauer, Phys. Rev. Lett. **95**, 016601 (2005).

[45] Y. Tserkovnyak, A. Brataas, and G. E. W. Bauer, Phys. Rev. Lett. **88**, 117601 (2002).

[46] H. Adachi, K. I. Uchida, E. Saitoh, and S. Maekawa, Rep. Prog. Phys. **76**, 036501 (2013).

[47] L. Chotorlishvili, Z. Toklikishvili, V. K. Dugaev, J. Barnaś, S. Trimper, and J. Berakdar, Phys. Rev. B **88**, 144429 (2013).

[48] X. Joyeux, T. Devolder, J.-V. Kim, Y. Gomez de la Torre, S. Eimer, and C. Chappert, J. Appl. Phys. **110**, 063915 (2011).

[49] L. Chotorlishvili, Z. Toklikishvili, S. R. Etesami, V. K. Dugaev, J. Barnaś, and J. Berakdar, J. Magn. Magn. Mater. **396**, 254 (2015).

[50] D. A. Garanin, Phys. Rev. B **55**, 3050 (1997).